Acoustic axes in weak triclinic anisotropy

Václav Vavryčuk

Geophysical Institute, Academy of Sciences of the Czech Republic, Boční II, 141 31 Praha 4, Czech Republic, E-mail: vv@ig.cas.cz

Abstract

Acoustic axes can exist even under an infinitesimally weak anisotropy, and occur when slowness surfaces of the *S*1 and *S*2 waves touch or intersect. The maximum number of isolated acoustic axes in weak triclinic anisotropy is 16 as in strong triclinic anisotropy. The directions of acoustic axes are calculated by solving two coupled polynomial equations in two variables. The order of the equations is six under strong anisotropy and reduces to five under weak anisotropy. The weak anisotropy approximation is particularly useful, when inverting for anisotropy from the directions of acoustic axes. The minimum number of acoustic axes, which can be inverted for weak anisotropy, is seven, and at the most 13 combinations of elastic parameters can be retrieved. Numerical tests have shown that the inversion is sufficiently accurate only for very weak anisotropy with strength less than 5%, and provided that the acoustic axes used in the inversion are determined with an accuracy better than 0.3°.

1. INTRODUCTION

Acoustic axes (singularities, degeneracies) are directions in anisotropic media, in which phase velocities of two or three plane waves (*P*, *S*1 or *S*2 waves) coincide. We distinguish several types of acoustic axes (Khatkevich 1963; Fedorov 1968; Khatkevich 1977; Alshits & Lothe 1979a; Crampin & Yedlin 1981; Grechka & Obolentseva 1993; Helbig 1994): they can form either single isolated points classified as kiss, conical or wedge singularities, or they can combine into line singularities. The maximum number of isolated acoustic axes is (Khatkevich 1963; Darinskij 1994, Boulanger & Hayes 1998; Mozhaev et al. 2001): 16 in monoclinic and orthorhombic symmetry, 13 in tetragonal symmetry, 10 in trigonal

symmetry, seven in cubic symmetry, and one in transverse isotropy. The directions of the acoustic axes are calculated by solving polynomial equations in one variable. The degree of the polynomials is six under monoclinic symmetry, or less under other symmetries, and its numerical solving does not pose any difficulty. The maximum number of isolated acoustic axes in triclinic anisotropy is also 16 as in monoclinic and orthorhombic symmetries (Holm 1992; Darinskij 1994; Vavryčuk 2004). However, the calculation of the directions of the acoustic axes is more involved. The directions are calculated by solving two coupled polynomial equations of the sixth order in two variables (Khatkevich 1963; Alshits & Lothe 1979a; Vavryčuk 2004). Obviously this implies that the positions of acoustic axes are complicated functions of anisotropy parameters.

Acoustic axes are very important, because they can cause anomalies in the shape of the slowness surface and singularities in the field of polarization vectors (Alshits & Lothe 1979b; Alshits et al. 1985; Shuvalov 1998; Fig.1). Acoustic axes are frequently associated with caustics and anti-caustics in the wave surface (Shuvalov & Every 1997; Wolfe 1998; Vavryčuk 2003a), with triplications and with energy focusing (Hurley & Wolfe 1985; Every 1986, 1988; Wolfe 1998). They also pose complications in tracing rays (Vavryčuk 2001, 2003b) and in wavefield modelling because of the coupling of waves (Chapman & Shearer 1989; Coates & Chapman 1990; Rümpker & Thomson 1994; Pšenčík 1998).

In general, anomalies observed in the directions of acoustic axes and in their vicinities appear, or they are more pronounced, under strong rather than weak anisotropy. For example, we can observe acoustic axes of the *P* and *S*1 waves or triple acoustic axes of the *P*, *S*1 and *S*2 waves under strong anisotropy, but only the acoustic axes of the *S*1 and *S*2 waves can be observed under weak anisotropy. Also triplications of the wave surface appear more frequently under strong rather than weak anisotropy. Under weak anisotropy, the shapes of slowness and wave surfaces and the behaviour of waves are usually much simpler and modelling of propagating waves is much easier. Importantly, weak anisotropy is not only a useful theoretical concept simplifying modelling of waves, but it is also a reasonable assumption valid for many real materials including most rocks and geological structures in the Earth (Thomsen 1986, Babuška & Cara 1991; Savage 1999).

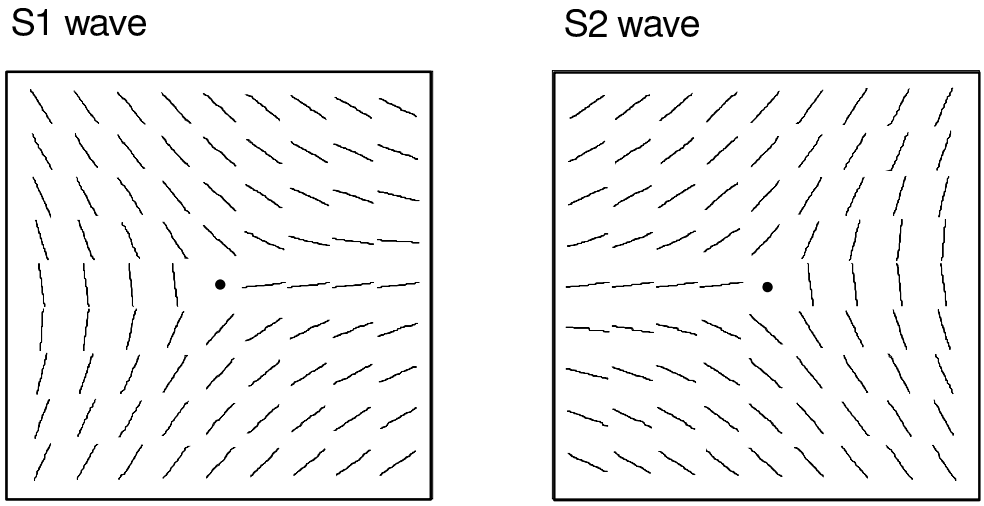

Figure 1. The field of polarization vectors on the slowness surfaces near a conical acoustic axis for the *S*1 and *S*2 waves. The polarization vectors are projected into the plane perpendicular to the acoustic axis. The field of polarization vectors is singular in the acoustic axis. The topological charge of the singularity is -1/2. The dot marks the position of the singularity.

For the reasons mentioned, we shall focus in this paper on studying the number and properties of acoustic axes in weak triclinic anisotropy. We shall apply the perturbation theory (Jech & Pšenčík 1989; Farra 2001; Vavryčuk 2003a) to check whether a rather complicated calculation of the number and directions of acoustic axes in triclinic anisotropy simplifies under weak anisotropy. We shall try to find specific properties of acoustic axes in weak anisotropy and to resolve whether the maximum number of singularities is reduced under weak anisotropy. Furthermore, we shall examine the possibility to invert for weak anisotropy parameters from the directions of acoustic axes and find out how many acoustic axes we need for a successful inversion for anisotropy.

2. ACOUSTIC AXES IN STRONG ANISOTROPY

2.1. System of equations

The Christoffel tensor $\mathbf{\Gamma}(\mathbf{n})$ is defined as (Fedorov 1968; Musgrave 1970; Červený 2001)

$$\Gamma_{jk}(\mathbf{n}) = a_{ijkl} n_i n_l \ , \tag{1}$$

where a_{ijkl} are the density-normalized elastic parameters and **n** is the unit vector defining the slowness direction. The Einstein summation convention over repeated subscripts is applied. For physically realizable media, the elastic parameters a_{ijkl} satisfy the stability conditions (Helbig 1994, eqs 5.5-5.10) and the Christoffel tensor $\mathbf{\Gamma}(\mathbf{n})$ is positive-definite for all directions **n**. The Christoffel tensor $\mathbf{\Gamma}(\mathbf{n})$ has three eigenvalues $G^{(M)}$ and three unit eigenvectors $\mathbf{g}^{(M)}$, which are calculated from

$$\Gamma_{jk} g_k^{(M)} = G^{(M)} g_j^{(M)} \ , M = 1,2,3 \ , \tag{2}$$

where M denotes the type of wave (P, $S1$ or $S2$). The eigenvalue corresponds to the squared phase velocity, $G = c^2$, and the eigenvector describes the polarization vector of the wave. Using the spectral decomposition of $\mathbf{\Gamma}(\mathbf{n})$

$$\Gamma_{jk} = G^{(1)} g_j^{(1)} g_k^{(1)} + G^{(2)} g_j^{(2)} g_k^{(2)} + G^{(3)} g_j^{(3)} g_k^{(3)} , \tag{3}$$

and applying the condition for the acoustic axis, $G^{(2)} = G^{(3)}$, we obtain

$$\Gamma_{jk} = \left(G^{(1)} - G^{(2)}\right) g_j^{(1)} g_k^{(1)} + G^{(2)} \delta_{jk} \ , \tag{4}$$

where δ_{jk} is the Kronecker delta and the following identity was used

$$\delta_{jk} = g_j^{(1)} g_k^{(1)} + g_j^{(2)} g_k^{(2)} + g_j^{(3)} g_k^{(3)} \ . \tag{5}$$

If $G^{(1)} > G^{(2)} = G^{(3)}$, the *S*1 and *S*2 phase velocities coincide at the acoustic axis, if $G^{(1)} < G^{(2)} = G^{(3)}$, the *P* and *S*1 phase velocities coincide at the acoustic axis. Equation (4) can be expressed as follows (Darinskij 1994):

$$a_{ijkl} s_i s_l = g_j g_k + \delta_{jk} \ , \tag{6}$$

where $\mathbf{s} = \mathbf{n} / \sqrt{G^{(2)}}$ is the slowness vector of the degenerate wave and $\mathbf{g} = \mathbf{g}^{(1)} \sqrt{\left(G^{(1)} - G^{(2)}\right) / G^{(2)}}$ is an eigenvector of the non-degenerate wave of a generally non-unit length. Vectors **s** and **g** may be real- or complex-valued. Equation (6) is a system of six quadratic equations in six unknowns: $\mathbf{s} = (s_1, s_2, s_3)^T$ and $\mathbf{g} = (g_1, g_2, g_3)^T$. The number of solutions is $2^6 = 64$. If we take into account that solutions of different signs: $\pm\mathbf{s}$, $\pm\mathbf{g}$, correspond to the same acoustic axis, the maximum number of acoustic axes is reduced from 64 to 16. This number comprises the solutions with real-valued as well as complex-valued slowness vector **s.** The real-valued/complex-valued solutions correspond to acoustic axes of homogeneous/inhomogeneous plane waves propagating in anisotropic media (see Vavryčuk 2004)

Eliminating eigenvalues and eigenvectors in eq. (4), we obtain (Darinskij 1994):

$$\Gamma_{11} - \frac{\Gamma_{12}\Gamma_{13}}{\Gamma_{23}} = \Gamma_{22} - \frac{\Gamma_{12}\Gamma_{23}}{\Gamma_{13}} = \Gamma_{33} - \frac{\Gamma_{13}\Gamma_{23}}{\Gamma_{12}} \ , \tag{7}$$

or alternatively (Khatkevich 1963):

$$(\Gamma_{11} - \Gamma_{22})\Gamma_{13}\Gamma_{23} - \Gamma_{12}\left(\Gamma_{13}^2 - \Gamma_{23}^2\right) = 0 \ , \tag{8a}$$

$$(\Gamma_{11} - \Gamma_{33})\Gamma_{12}\Gamma_{23} - \Gamma_{13}\left(\Gamma_{12}^2 - \Gamma_{23}^2\right) = 0 \ , \tag{8b}$$

$$(\Gamma_{22} - \Gamma_{33})\Gamma_{12}\Gamma_{13} - \Gamma_{23}\left(\Gamma_{12}^2 - \Gamma_{13}^2\right) = 0 \ . \tag{8c}$$

Equations (8a-c) are suitable for calculating the acoustic axes numerically. They represent a system of sixth-order equations for three unknown components of the unit direction vector **n**: n_1, n_2 and n_3. The three equations (8a-c) are not independent, hence we solve only two of them. We obtain 72 solutions, which are generally complex-valued. Taking into account that $\pm\mathbf{n}$ describes the same direction, the number of directions reduces from 72 to 36.

2.2. Spurious directions

Since eq. (6) yields only 16 acoustic axes, 20 of the 36 directions calculated from (8) must be spurious and do not describe acoustic axes. In fact, the spurious directions were incorporated into the solution, when eq. (7) was multiplied by terms $\Gamma_{12}\Gamma_{13}$, $\Gamma_{12}\Gamma_{23}$ or $\Gamma_{13}\Gamma_{23}$ in order to derive eq. (8). Therefore, we should eliminate from the solutions of eq. (8a-c) the directions, for which

$$\Gamma_{13}=0 \text{ and } \Gamma_{23}=0, \tag{9a}$$

or

$$\Gamma_{12}=0 \text{ and } \Gamma_{23}=0, \tag{9b}$$

or

$$\Gamma_{12}=0 \text{ and } \Gamma_{13}=0. \tag{9c}$$

Equations (9a-c) describe three systems of quadratic equations, each of them having eight solutions which reduce to four directions, if different signs of **n** are omitted. Hence, we obtained a total of 12 spurious directions. Furthermore, eight of the 12 spurious directions appear in eq. (8) twice. Which 8 spurious directions are doubled, depends on the pair of eqs (8a-c) we actually solve. For example, in solving eqs (8a-b), the solutions of eq. (9a) and (9b) are doubled; in solving eqs (8b-c), the solutions of eqs (9b) and (9c) are doubled. Hence, the total number of spurious directions in eq. (8) is 20. This confirms that only 16 acoustic axes can exist in triclinic anisotropy.

3. ACOUSTIC AXES IN WEAK ANISOTROPY

3.1. Weak anisotropy expansion

Weak triclinic anisotropy with elastic parameters a_{ijkl} is obtained by perturbing an isotropic medium in the following way:

$$a_{ijkl} = a^0_{ijkl} + \varepsilon b_{ijkl}\,, \tag{10}$$

where

$$a^0_{ijkl} = \lambda\delta_{ij}\delta_{kl} + \mu\left(\delta_{ik}\delta_{jl} + \delta_{il}\delta_{jk}\right)\,, \tag{11}$$

Parameters λ and μ define the Lamé coefficients of an isotropic background medium, tensor b_{ijkl} defines the perturbations from isotropy into triclinic anisotropy, and ε is a small quantity which measures anisotropy strength. For any weak triclinic anisotropy, the isotropic background medium can be chosen so that $b_{3333} = 0$ and $b_{1212} = 0$. These constraints are applied in all the following equations. Hence, the weakly anisotropic triclinic medium is described by 21 elastic parameters, two of them define the isotropic background and 19 of them define the perturbation to anisotropy.

For $\varepsilon = 0$ in (10), weak anisotropy reduces to isotropy. The Christoffel tensor $\mathbf{\Gamma}$ in (1) is degenerate with eigenvalues $G^P = \lambda + 2\mu$ and $G^S \equiv G^{S1} = G^{S2} = \mu$, which are independent of direction **n.** Consequently, the *P*- and *S*-wave slowness surfaces are fully detached, $G^P > G^S$, and the *S*1 and *S*2 waves have coincident phase velocities in all directions **n,** $G^{S1} = G^{S2}$. For small ε, the *P* wave remains detached from the *S*1 and *S*2 waves, but the global degeneracy of the *S*1 and *S*2 waves is removed, and the phase velocities of the *S*1 and *S*2 waves can coincide only in selected directions (see Fig. 2). Hence, under weak anisotropy we can observe acoustic axes of the *S*1 and *S*2 waves, but not the acoustic axes of the *P* and *S*1 waves, or the triple acoustic axes of the *P*, *S*1 and *S*2 waves.

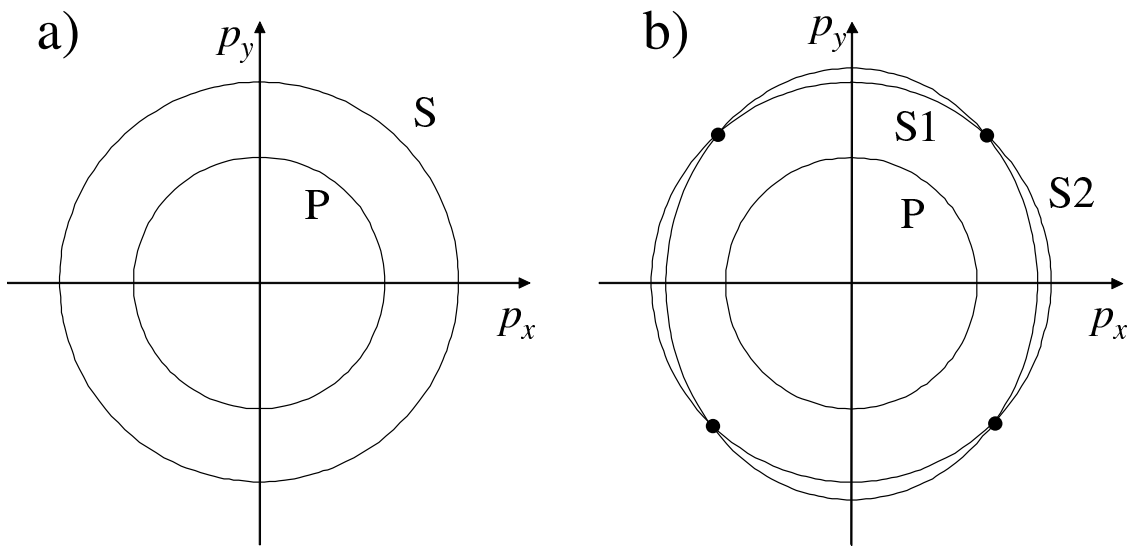

Figure 2. A sketch of slowness surfaces for *P* and *S* waves for isotropic media (a) and for *P*, *S*1 and *S*2 waves for weakly anisotropic media (b). The dots in (b) mark the positions of the acoustic axes.

3.2. System of equations

Inserting (10-11) into (8a) we obtain:

$$\varepsilon(\lambda+\mu)^2 P_1(b_{ijkl},n_1,n_2,n_3)+\varepsilon^2(\lambda+\mu)P_2(b_{ijkl},n_1,n_2,n_3)+\varepsilon^3 P_3(b_{ijkl},n_1,n_2,n_3)=0, \qquad (12a)$$

$$\varepsilon(\lambda+\mu)^2 Q_1(b_{ijkl},n_1,n_2,n_3)+\varepsilon^2(\lambda+\mu)Q_2(b_{ijkl},n_1,n_2,n_3)+\varepsilon^3 Q_3(b_{ijkl},n_1,n_2,n_3)=0, \qquad (12b)$$

$$\varepsilon(\lambda+\mu)^2 R_1(b_{ijkl},n_1,n_2,n_3)+\varepsilon^2(\lambda+\mu)R_2(b_{ijkl},n_1,n_2,n_3)+\varepsilon^3 R_3(b_{ijkl},n_1,n_2,n_3)=0, \qquad (12c)$$

where polynomials P_1, Q_1 and R_1 are of the first order, polynomials P_2, Q_2 and R_2 are of the second order, and P_3, Q_3 and R_3 are polynomials of the third order in b_{ijkl}.

If we assume $\varepsilon/(\lambda+\mu)\to 0$ (but not equal to zero), we can neglect the higher-order terms in ε in equations (12a-c) and retain only the linear terms in ε. We then obtain:

$$P_1\left(b_{ijkl}, n_1, n_2, n_3\right) = 0, \tag{13a}$$

$$Q_1\left(b_{ijkl}, n_1, n_2, n_3\right) = 0, \tag{13b}$$

$$R_1\left(b_{ijkl}, n_1, n_2, n_3\right) = 0. \tag{13c}$$

Polynomials P_1, Q_1 and R_1 are homogeneous polynomials of the sixth order. They can be expressed as follows:

$$P_1 = n_3 p_{ij} n_1^i n_2^j n_3^{5-i-j},\ Q_1 = n_2 q_{ij} n_1^i n_2^j n_3^{5-i-j},\ R_1 = n_1 r_{ij} n_1^i n_2^j n_3^{5-i-j}, \tag{14}$$

where summation over repeated indices is applied. Indices i and j run from 0 to 5, and their sum is less than or equal to 5. Coefficients p_{ij}, q_{ij} and r_{ij} are presented in Appendix A. If we choose a coordinate system, in which no acoustic axis lies in the coordinate planes, then equations (13a-c) simplify as follows

$$p_{ij} n_1^i n_2^j n_3^{5-i-j} = 0, \tag{15a}$$

$$q_{ij} n_1^i n_2^j n_3^{5-i-j} = 0, \tag{15b}$$

$$r_{ij} n_1^i n_2^j n_3^{5-i-j} = 0, \tag{15c}$$

where $k = 5 - i - j$. The equations are homogeneous polynomial equations of the fifth order in three unknown components of the unit vector **n**. The equations can be transformed into inhomogeneous polynomial equations of the fifth order for two unknowns u and v:

$$p_{ij} u^i v^j = 0, \tag{16a}$$

$$q_{ij} u^i v^j = 0, \tag{16b}$$

$$r_{ij} u^i v^j = 0, \tag{16c}$$

where $u = n_1 / n_3$ and $v = n_2 / n_3$, and we assume no acoustic axis in the x_1–x_2 plane ($n_3 = 0$). Indices *i* and *j* run from zero to five and their sum is less than or equal to five.

Equations (16a-c) are not independent, hence we solve only two of them. In solving equations (16a-b) or (16a-c), we obtain 25 real- or complex-valued solutions. In solving equations (16b-c), we obtain 22 real- or complex-valued solutions. In both cases, the solutions comprise the true acoustic axes as well as the spurious directions.

3.3. Spurious directions

To identify and eliminate the spurious directions from the solutions of (16a-c), we have to solve complementary equations similar to equations (9a-c) designed for strong anisotropy. Expressing the Christoffel tensor in (9a-c) for weak anisotropy and keeping the leading terms only, we obtain:

$$(\lambda + \mu) n_1 n_3 = 0 \quad \text{and} \quad (\lambda + \mu) n_2 n_3 = 0, \tag{17a}$$

or

$$(\lambda + \mu) n_1 n_2 = 0 \quad \text{and} \quad (\lambda + \mu) n_2 n_3 = 0, \tag{17b}$$

or

$$(\lambda + \mu) n_1 n_2 = 0 \quad \text{and} \quad (\lambda + \mu) n_1 n_3 = 0. \tag{17c}$$

The number and positions of the spurious directions depend on the choice of the pair of equations (17a-c) we actually solve. If we solve equations (17a) and (17b) or equations (17a) and (17c), we shall find that the spurious directions lie in all three coordinate planes: x_1–x_2, x_1–x_3 and x_2–x_3. If we solve equations (17b) and (17c), the spurious directions lie only in two coordinate planes: x_1–x_3 and x_2–x_3. It can be proved that each coordinate plane contains three spurious solutions, so that a total nine spurious solutions is obtained in

solving equations (17a) and (17b), or in solving equations (17a) and (17c), and six spurious solutions in solving equations (17b) and (17c).

Hence, if we calculate the acoustic axes by solving (16a-b) we obtain 25 solutions from which we have to eliminate nine spurious directions obtained by solving equations (17a-b). We proceed similarly with pairs (16a) and (16c), or (17a) and (17c). In solving (16b) and (16c), we obtain 22 solutions from which we have to eliminate six spurious solutions by solving (17b) and (17c). We thus find that the maximum number of acoustic axes in weak triclinic anisotropy is 16 in any case. This implies that weak triclinic anisotropy is characterized by the same maximum number of acoustic axes as strong triclinic anisotropy.

As an example of weak triclinic anisotropy with 16 acoustic axes we give the following perturbation matrix:

$$\mathbf{b} = \begin{bmatrix} -0.35 & -0.52 & -0.02 & -0.01 & 0.22 & -0.01 \\ & -0.57 & -0.04 & -0.02 & 0.43 & -0.01 \\ & & 0 & 0.01 & 0.26 & -0.01 \\ & & & -0.59 & -0.01 & 0.21 \\ & & & & -0.55 & 0.01 \\ & & & & & 0 \end{bmatrix}, \tag{18}$$

expressed in two-index notation (see Musgrave 1970, eq. 3.13.4). This anisotropy has 16 acoustic axes not only for infinitesimally small anisotropy strength, but also for anisotropy with ε up to 0.2 assuming $\lambda = 1$ and $\mu = 1$ in equations (10-11). The positions of the acoustic axes on the sphere are shown in Fig. 3.

3.4. Numerical calculation of acoustic axes

The exact directions of acoustic axes in weak as well as strong triclinic anisotropy can be conveniently calculated by solving modified equations (12a-c). The modification lies in dividing (12a-c) by ε. These are homogeneous polynomial equations of the sixth order in three unknown components n_1, n_2 and n_3 of the unit direction vector **n**. Using the substitutions $u = n_1 / n_3$ and $v = n_2 / n_3$, we obtain inhomogeneous polynomial equations of the sixth order in unknowns u and v. The roots of the equations can be calculated, for

example, using Gröbner bases (Fröberg 1997), implemented in symbolic algebra packages. Solving modified equations (12a-c) we obtain 36 solutions, from which we have to exclude 20 spurious solutions defined by eqs (9a-c). To identify and eliminate the spurious solutions, we can either solve eqs (9a-c) or we can simply check, at which of the 36 directions calculated from eqs (12a-c) the Christoffel tensor is non-degenerate. Using this approach, we obtain the exact real as well as complex acoustic axes in triclinic media with any strength of anisotropy. On the contrary, equations (8a-c), which are equivalent to (12a-c), are suitable for calculating acoustic axes under strong rather than weak anisotropy. The reason is that (8a-c) can fail if triclinic anisotropy is extremely weak. In this case, the left-hand sides of (8a-c) are very close to zero for all directions **n**, and the solution can be distorted by numerical errors.

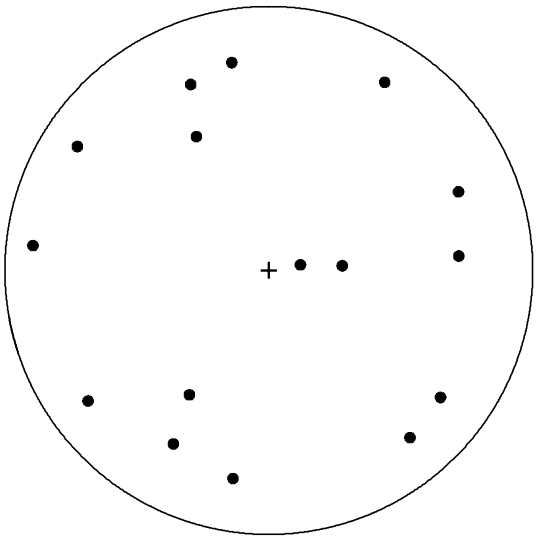

Figure 3. A polar plot of positions of acoustic axes for a weak triclinic anisotropy with 16 acoustic axes. The vertical axis is marked by the plus sign. For parameters of anisotropy parameters b_{ijkl}, see (18). Other parameters: $\lambda = 1$, $\mu = 1$, and $\varepsilon = 0.01$.

The approximate directions of acoustic axes in weak triclinic anisotropy can be conveniently calculated using eqs (16a-c). The spurious directions can be eliminated by solving eqs (17a-c). As mentioned, equations (16a-c) are inhomogeneous polynomial

equations of the fifth order in unknowns u and v. The roots of the equations can be calculated similarly as for strong anisotropy using Gröbner bases (Fröberg 1997), implemented in symbolic algebra packages. The weak anisotropy approximation has the following advantages: First, the fifth-order equations are solved faster than the sixth-order equations. Second, equations (16a-c) are much simpler and more easily to code than equations (12a-c), because we neglect rather long and complex polynomials P_2, Q_2, R_2, P_3, Q_3 and R_3. Third, equations (16a-c) can be used for inversion for anisotropy from known directions of acoustic axes, see the next section.

For media with a higher symmetry, it is not convenient to use equations (12a-c) and (17a-c) for finding the acoustic axes, because they are unnecessarily complicated and they may even fail when the true or spurious solutions are not isolated. Instead, much simpler systems of algebraic equations designed for each specific symmetry are used (Boulanger & Hayes 1998).

4. INVERSION FOR ANISOTROPY

The equations for the directions of acoustics axes in anisotropic media are non-linear functions of elastic parameters a_{ijkl}. However, under weak anisotropy, the equations can be linearized. The linearized equations are much simpler, and thus more suitable for solving the inverse problem. Hereinafter, we shall linearize equation (6) derived by Darinskij (1994) as well as equations (8a-c) derived by Khatkevich (1963). On numerical examples we shall calculate anisotropy from the directions of acoustic axes using both approaches and compare their accuracy.

4.1. Linearization of the Khatkevich equations

Equations (15a-c) represent the sought linearized form of the Khatkevich equations (8a-c). The equations can be used in the forward problem to seek the directions of acoustic axes from known anisotropy parameters, but they can also be used in the inverse problem to calculate anisotropy parameters from the known directions of acoustic axes. As expected, the equations cannot be used for inverting for the isotropic background, only perturbations into anisotropy can be calculated. In the inversion for anisotropy, the equations represent a

system of linear homogeneous equations for coefficients of perturbation matrix b_{ijkl}. The matrix contains 19 parameters (the reader is reminded that parameters b_{33} and b_{66} were fixed to be zero), but not all of them stand in eqs (15a-c) independently. Some of the parameters appear in the equations in combinations, hence the inversion can yield only the following 14 parameters:

$$b_{44},\ b_{45},\ b_{46},\ b_{55},\ b_{56},\ b_{11}-2b_{13},\ b_{22}-2b_{23},\ b_{34}-b_{14},\ b_{34}-b_{24},\ b_{35}-b_{15},\ b_{35}-b_{25},\ b_{36}-b_{16},\ b_{36}-b_{26},\ b_{23}+b_{13}-b_{12}. \tag{19}$$

Since the system of equations is homogeneous, one parameter must always be fixed to get a non-trivial solution. Thus we cannot retrieve absolute values, but only normalized values of the parameters. In other words, we cannot invert for strength of anisotropy.

Since only two equations of (8a-c) are independent, we have to know at least seven directions of acoustic axes to obtain a properly determined system of equations. For seven acoustic axes, we obtain 14 equations, one of which one can be omitted (to get 13 equations for 13 unknowns). If we know a smaller number of axes, the system of equations is underdetermined and additional knowledge on anisotropy must be supplied for the system to be solvable. For example, phase velocities or polarization vectors of *P* waves at acoustic axes can serve as additional information. If we know the directions of seven or more acoustic axes, the problem is overdetermined and anisotropy can be calculated using the standard least-squares method.

Equations (15a-c) can be expressed as follows:

$$\mathbf{A}\mathbf{x} = \mathbf{c}, \tag{20}$$

where

$$\mathbf{x} = \frac{1}{b_{44}}[b_{45}, b_{46}, b_{55}, b_{56}, b_{11}-2b_{13}, b_{22}-2b_{23}, b_{34}-b_{14}, b_{34}-b_{24}, b_{35}-b_{15}, b_{35}-b_{25}, b_{36}-b_{16}, b_{36}-b_{26}, b_{23}+b_{13}-b_{12}]^T \tag{21}$$

is the 13x1 vector of unknown elastic parameters defining weak triclinic anisotropy, and **A** is the 2*N*x13 matrix and **c** is the 2*N*x1 vector, which are defined as follows

$$\mathbf{A}=\begin{bmatrix}\mathbf{A}^{(1)}\\ \mathbf{A}^{(2)}\\ \vdots\\ \mathbf{A}^{(N)}\end{bmatrix},\quad \mathbf{c}=\begin{bmatrix}\mathbf{c}^{(1)}\\ \mathbf{c}^{(2)}\\ \vdots\\ \mathbf{c}^{(N)}\end{bmatrix}. \tag{22}$$

Quantities $\mathbf{A}^{(i)}$ and $\mathbf{c}^{(i)}$ are the 2x13 matrix and 2x1 vector, respectively, which are calculated for the *i*th acoustic axis (see Appendix C). The elastic parameters come out as

$$\mathbf{x}=\mathbf{A}^{-1}\mathbf{c} \tag{23}$$

where $\mathbf{A}^{-1}$ stands for the least-squares inversion of matrix **A**. As mentioned, eq. (23) is solvable provided $N\geq 7$ (**A** is the 14x13 matrix). If $N<7$, we have to complement eq. (20) by other equations for the inversion for anisotropy to be feasible.

4.2. Linearization of the Darinskij equations

Another possibility of inverting for anisotropy is to linearize the Darinskij equations (6). To do so we have to linearize the equations for eigenvalues *G* and eigenvectors **g** for the Christoffel tensor **Γ** along an acoustic axis (see Jech & Pšenčík 1989; Vavryčuk 2003a):

$$G^P \cong a_{ijkl}n_in_jn_kn_l=\alpha^2+\varepsilon\, b_{ijkl}n_in_jn_kn_l, \tag{24}$$

$$G^S=\frac{1}{2}\left(\Gamma_{ii}-G^P\right)\cong\frac{1}{2}\left(a_{ijki}n_jn_k-a_{ljkm}n_jn_kn_ln_m\right)=\beta^2+\frac{1}{2}\varepsilon\, b_{ljkm}n_jn_k\left(\delta_{lm}-n_ln_m\right), \tag{25}$$

$$g_i^P\cong n_i+\frac{1}{\alpha^2-\beta^2}\varepsilon\, b_{jopk}n_on_pn_j\left(\delta_{ik}-n_in_k\right), \tag{26}$$

where we have used

$$\Gamma_{ii} = \mathrm{Tr}(\Gamma) = G^P + G^{S1} + G^{S2} = G^P + 2G^S , \tag{27}$$

$$\alpha^2 = \lambda + 2\mu , \; \beta^2 = \mu . \tag{28}$$

Quantities α and β denote the *P* and *S* velocities in the isotropic background, G^P and G^S ($G^S = G^{S1} = G^{S2}$) are eigenvalues of the Christoffel matrix $\mathbf{\Gamma}$ for the *P* waves and for the degenerate *S* waves along the acoustic axis, and vector $\mathbf{g}^P$ is the *P*-wave polarization vector along the acoustic axis. Consequently, we obtain

$$G^P - G^S \cong \alpha^2 - \beta^2 + \frac{1}{2}\varepsilon b_{ljkm} n_j n_k (3 n_l n_m - \delta_{lm}) , \tag{29}$$

$$g_i^P g_l^P \cong n_i n_l + \frac{1}{\alpha^2 - \beta^2}\varepsilon b_{jopk} n_o n_p n_j (\delta_{ik} n_l + \delta_{lk} n_i - 2 n_i n_k n_l) , \tag{30}$$

Inserting (29) and (30) into (6) we obtain

$$b_{pjkr} n_p n_r (2\delta_{ij}\delta_{lk} - \delta_{jk}\delta_{il} + n_i n_l \delta_{jk} + n_j n_k \delta_{il} - 2 n_j n_l \delta_{ik} - 2 n_i n_j \delta_{lk} + n_j n_k n_i n_l) \cong 0 , \; i,l = 1,2,3, \tag{31}$$

where we have omitted all higher-order terms of ε.

Inserting the known direction vector $\mathbf{n}$ for one acoustic axis into (31) we obtain six linear equations, but only two of them are independent. A detailed analysis reveals that the anisotropy parameters b_{ijkl} do not stand in equation (31) independently, but in 14 combinations, which are the same as for the linearized Khatkevich equations, see (19). As the equations are homogeneous, we are able to invert for 13 parameters only. For this we need at least 13 independent equations, which can be obtained by inserting the directions of seven acoustic axes. In this case we obtain 14 equations, so that one equation can be omitted. Hence, the minimum number of acoustic axes necessary for the inversion is the same as for the approach that uses the linearized Khatkevich equations. Mathematically, anisotropy is calculated using a similar system of linear equations as (23) derived for the Khatkevich equations with matrix $\mathbf{A}$ and vector $\mathbf{c}$ specified in Appendix D.

4.3. Numerical tests

In this section, we shall test the efficiency of the inversion for anisotropy using the linearized Khatkevich and Darinskij equations. We shall generate synthetic triclinic anisotropy and calculate the number and directions of acoustic axes. We shall then invert from the axes for anisotropy and compare the results with the exact values.

We shall perform the following tests: (1) We shall invert for anisotropy of varying strength to determine the range of applicability of the linearized inversion. (2) The directions of the acoustic axes will be specified with a varying accuracy to test the sensitivity of the inversion to noise in the data. From this we shall estimate the minimum accuracy required to measure the directions in experiments. (3) We shall compare the accuracy of the results obtained using the Khatkevich and Darinskij equations to resolve which method is more efficient.

Weak triclinic anisotropy is calculated by equations (10) and (11) with the Lamé coefficients $\lambda = 1$, and $\mu = 1$, and with the following perturbation matrix expressed in the two-index notation:

$$\mathbf{b} = \begin{bmatrix} 1.26 & -1.02 & -1.11 & 0.69 & 0.48 & 0.78 \\ & -1.14 & 0.81 & 0.51 & 1.17 & -0.66 \\ & & 0 & -0.24 & -0.84 & -1.38 \\ & & & 0.96 & -1.23 & 1.08 \\ & & & & 1.23 & -0.45 \\ & & & & & 0 \end{bmatrix}. \tag{32}$$

Inserting (32) into (21) we obtain the following exact values of the anisotropy parameters, for which we shall invert

$$\mathbf{x}^{exact} = \left[-1.281, 1.125, 1.281, -0.469, 3.625, -2.875, -0.969, -0.781, -1.375, -2.094, -2.250, -0.750, 0.750\right] \tag{33}$$

Parameter ε in (10) runs from 0.0001 to 0.1, it thus covers a wide range of anisotropy strength. The anisotropy has eight real-valued acoustic axes and their directions depend only very slightly on ε. For directions of acoustic axes for $\varepsilon = 0.1$, see Fig. 4 and Tab. 1.

We invert for anisotropy from the directions of all eight acoustic axes, hence, we use 16 independent equations in (20) and (23). Matrix **A** and vector **c** are specified in Appendix C for the Khatkevich equations and in Appendix D for the Darinskij equations. We invert from the exact directions of the acoustic axes (see Tab. 1) as well as from the directions, which slightly deviate from the exact ones, to test the stability of the inversion. The deviations were generated randomly and varied within a wide range of values to mimic observations of different accuracy. For each specific accuracy, 1000 realizations of noisy directions of acoustic axes were generated and inverted for anisotropy. The relative error of each inversion was calculated as the average error e of the calculated elastic parameters x_i^{aprox}, i=1,…,13,

$$e = \frac{1}{13}\sum_{i=1}^{13} \frac{x_i^{exact} - x_i^{aprox}}{x_i^{exact}} \cdot 100\% \ . \tag{34}$$

The relative error of the inversions for each accuracy of the directions of acoustic axes was calculated as the average error over all 1000 random realizations of noisy directions.

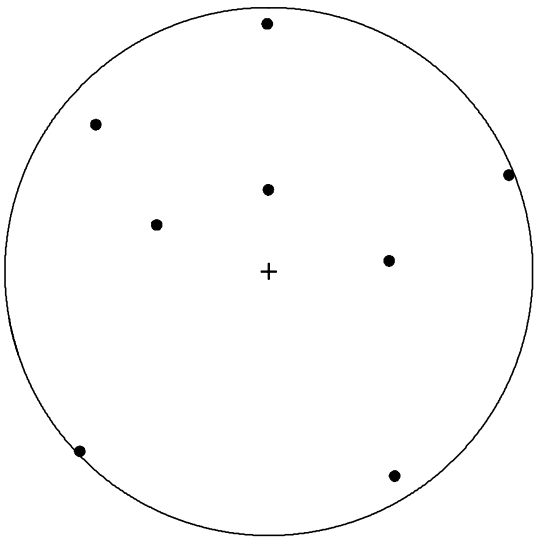

Figure 4. A polar plot of positions of acoustic axes for a weak triclinic anisotropy used in the numerical tests. The vertical axis is marked by the plus sign. For parameters of anisotropy parameters b_{ijkl}, see (32). Other parameters: $\lambda = 1$, $\mu = 1$, and $\varepsilon = 0.1$.

Table 1. Positions of real-valued acoustic axes

No.	n_1	n_2	n_3
1	-0.71633651	-0.68125083	0.15086190
2	0.47672546	-0.77512142	0.41463190
3	0.45580623	0.03994563	0.88918223
4	-0.42485819	0.17634656	0.88791746
5	-0.00165142	0.30916450	0.95100714
6	-0.65567544	0.55638510	0.51041683
7	0.90968347	0.36506007	0.19800793
8	-0.00622865	0.93770784	0.34736899

Figure 5 shows the relative error of the inversion as a function of the *P*-wave anisotropy strength a^P calculated as

$$a^P = \frac{c^{\max} - c^{\min}}{\bar{c}} \cdot 100\% , \tag{35}$$

where $c^{\max}$, $c^{\min}$, and $\bar{c}$ mean the maximum, minimum and average phase velocity of the *P* wave over all directions of propagation. The relative error is shown for the exact directions of the acoustic axes (curve a) and for the directions of limited accuracy (curves b-g). The error of the inversion increases with increasing strength of anisotropy. If the anisotropy strength is higher than 10%, the inversion fails. This follows from using linearized equations applicable only to weak anisotropy. As expected, the error also increases with decreasing accuracy of the directions of acoustic axes. If an average deviation between the exact and noisy directions of acoustic axes used in the inversion is higher than 1° (curves f-g), the inversion yields errors higher than 10% for the Darinskij equations and errors higher than 50% for the Khatkevich equations, irrespective of the strength of anisotropy. It points to the rather high demands of the inversion on the accuracy of acoustic axes. To get results with an accuracy better than 5% using the Khatkevich equations, the acoustic axes must be determined with an accuracy better than 0.1° and the

anisotropy strength must be less than 1%. If we use the Darinskij equations, the accuracy of the acoustic axes must be better than 0.3°, and the anisotropy strength must be less than 3%. The strong dependence of the inversion accuracy on the accuracy of the acoustic axes and on anisotropy strength is also shown in Fig. 6, depicting the inversion error as a function of the average deviation of the acoustic axes from the exact directions. The figure shows that even for extremely weak anisotropy (curve a), the inversion yields errors higher than 5% if the accuracy of the acoustic axes is less than 0.1° for the Khatkevich equations and less than 0.5° for the Darinskij equations. This also indicates that the Darinskij equations are more efficient than the Khatkevich equations. A detailed comparison of the efficiency of both approaches is shown in Fig. 7. The figure shows the inversion error as a function of the *P*-wave anisotropy strength when inverting exact acoustic axes (upper plots) and noisy acoustic axes with an average deviation of 0.1°. The inversion error for the Khakevich equations is more than 3 times higher than for the Darinskij equations, irrespective of the anisotropy strength and the accuracy of the acoustic axes. Hence, the Darinskij equations are definitely preferable for the inversion.

4. CONCLUSIONS

Acoustic axes can exist even under an infinitesimally weak anisotropy, and occur when slowness surfaces of the *S*1 and *S*2 waves touch or intersect. The maximum number of isolated acoustic axes in weak triclinic anisotropy is 16 as in strong triclinic anisotropy, hence a weak anisotropy condition does not reduce the maximum number of acoustic axes. However, media with 16 real-valued acoustic axes are very rare; the most frequent number of acoustic axes in weak triclinic anisotropy is much less, ranging between four to six (Vavryčuk 2004).

The directions of acoustic axes for strong anisotropy are calculated by solving two coupled polynomial equations of the sixth order in two variables. Under the condition of weak anisotropy, the order of the equations is reduced from six to five. Hence applying *the weak anisotropy approximation is not very beneficial, because it does not simplify the calculation of acoustic axes substantially*.

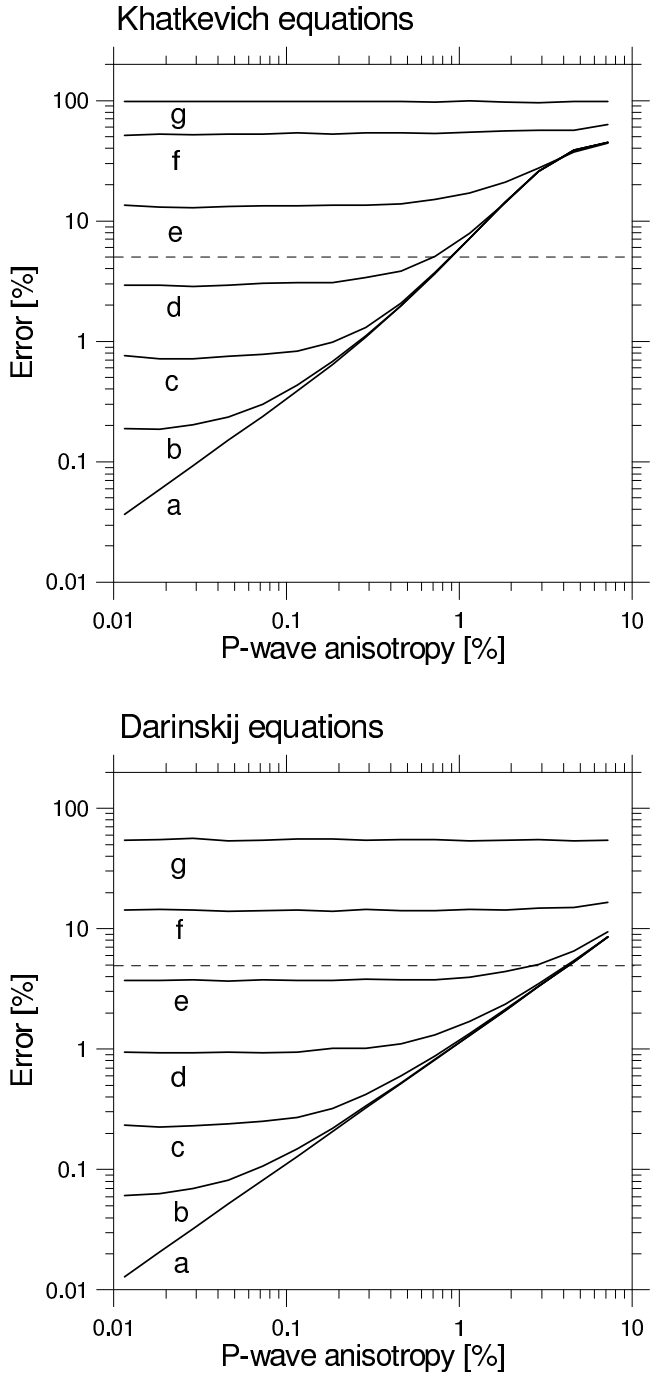

Figure 5. Errors of calculated elastic parameters as a function of *P*-wave anisotropy strength. The inversion was performed using exact (a) and approximate (b-g) directions of acoustic axes. The average deviation of the approximate directions from the exact was (in degrees): 0.0043 (b), 0.017 (c), 0.069 (d), 0.27 (e), 1.1 (f), and 4.3 (g). The dashed line shows the error threshold of 5%.

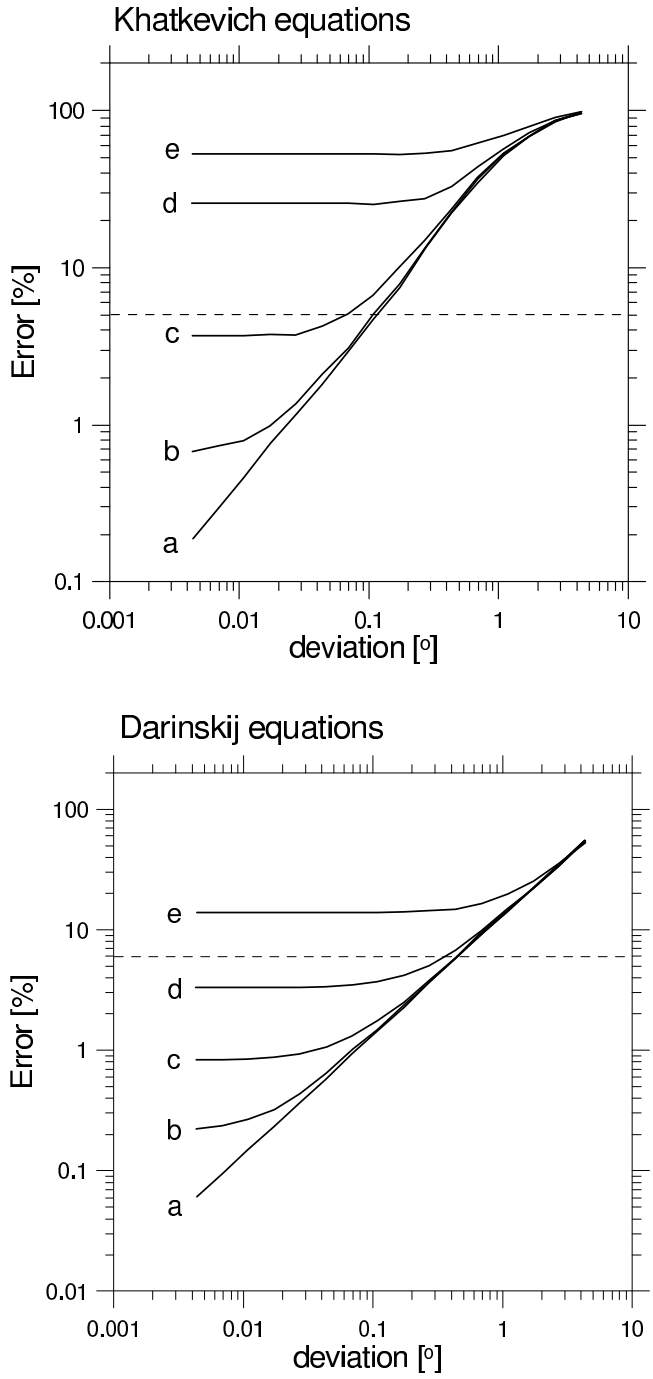

Figure 6. Errors of calculated elastic parameters as a function of the deviation of approximate directions of acoustic axes used in the inversion from the exact directions. The *P*-wave anisotropy strength is 0.012% (a), 0.18% (b), 0.73% (c), 2.9% (d), and 11% (e). The dashed line shows the error threshold of 5%.

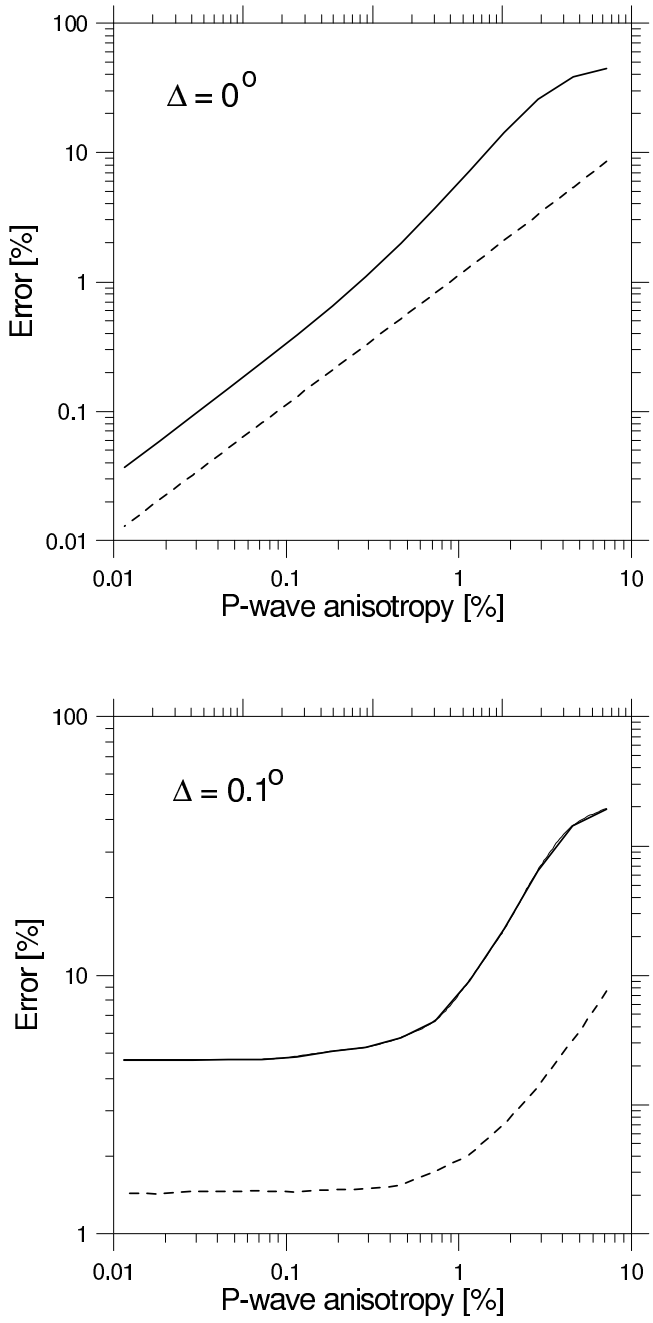

Figure 7. Errors of calculated elastic parameters as a function of the *P*-wave anisotropy strength for the Khatkevich (solid line) and Darinskij (dashed line) equations. The inversion was performed using exact (upper plot) and approximate (lower plot) directions of acoustic axes. The average deviation Δ of approximate directions was 0.1°.

On the other hand, applying the *weak anisotropy approximation is advantageous in inverting for anisotropy from the directions of acoustic axes*. The minimum number of acoustic axes, which can be inverted for weak anisotropy, is seven, and we can retrieve 13 combinations of elastic parameters. Numerical tests have shown that the inversion is applicable only to very weak anisotropy with strength of less than 5%, provided that the acoustic axes used in the inversion are determined with an accuracy better than 0.3°. In this case the inversion yields an average error for elastic parameters of less than 5%. The tests have also revealed significant differences when using different linearized equations: the linearized Darinskij equations are three times as efficient as the linearized Khatkevich equations, and thus are preferable in numerical calculations.

If the studied weak anisotropy possesses less than seven real-valued acoustic axes, we cannot invert for anisotropy from acoustic axes only. In this case, we have to incorporate additional equations in the inversion, for example, equations obtained from measurements of phase velocities in selected directions.

References

Alshits, V.I. & Lothe, J., 1979a. Elastic waves in triclinic crystals. I. General theory and the degeneracy problem, *Sov. Phys. Crystallogr.*, **24**, 387-392.

Alshits, V.I. & Lothe, J., 1979b. Elastic waves in triclinic crystals. II. Topology of polarization fields and some general theorems, *Sov. Phys. Crystallogr.*, **24**, 393-398.

Alshits, V.I., Sarychev, A.V. & Shuvalov, A.L., 1985. Classification of degeneracies and analysis of their stability in the theory of elastic waves in crystals, *J. Exper. Theor. Phys.*, **89**, 922-938 (in Russian).

Babuška, V., and M. Cara, *Seismic Anisotropy in the Earth*, Kluwer Academic Publishers, London, 1991.

Boulanger, Ph. & Hayes, M., 1998. Acoustic axes for elastic waves in crystals: theory and applications, *Proc. R. Soc. Lond.*, **A 454**, 2323-2346.

Červený, V., 2001. *Seismic Ray Theory*, Cambridge University Press, Cambridge.

Coates, R.T. & Chapman, C.H., 1990. Quasi-shear wave coupling in weakly anisotropic 3-D media, *Geophys. J. Int.*, **103**, 301-320.

Crampin, S. & Yedlin, M., 1981. Shear-wave singularities of wave propagation in anisotropic media, *J. Geophys.*, **49**, 43-46.

Darinskij, B.M., 1994. Acoustic axes in crystals, *Crystallogr. Rep.*, **39**, 697-703.

Every, A.G., 1986. Formation of phonon-focusing caustics in crystals, *Phys. Rev. B*, **34**, 2852-2862.

Every, A.G., 1988. Classification of the phonon-focusing patterns of tetragonal crystals, *Phys. Rev. B,* **37**, 9964-9977.

Farra, V., 2001. High-order perturbations of the phase velocity and polarization of qP and qS waves in anisotropic media, *Geophys. J. Int.*, **147**, 93-104.

Fedorov, F.I., 1968. *Theory of Elastic Waves in Crystals*, Plenum Press, New York.

Fröberg, R., 1997. *An Introduction to Gröbner Bases*, John Wiley, New York.

Grechka, V.Yu. & Obolentseva, I.R., 1993. Geometrical structure of shear wave surfaces near singularity directions in anisotropic media, *Geophys. J. Int.*, **115**, 609-616.

Helbig, K., 1994. *Foundations of Anisotropy for Exploration Seismics*, Pergamon, New York.

Holm, P., 1992. Generic elastic media, *Physica Scripta*, **T44**, 122-127.

Hurley, D.C. & Wolfe, J.P., 1985. Phonon focusing in cubic crystals, *Phys. Rev. B*, **32**, 2568-2587.

Jech, J. & Pšenčík, I., 1989. First-order perturbation method for anisotropic media, *Geophys. J. Int.*, **99**, 369-376.

Khatkevich, A.G., 1963. Acoustic axes in crystals, *Sov. Phys. Crystallogr.*, **7**, 601-604.

Khatkevich, A.G., 1977. Classification of crystals by acoustic properties, *Sov. Phys. Crystallogr.*, **22**, 701-705.

Mozhaev, V.G., Bosia, F. & Weihnacht, M., 2001. Oblique acoustic axes in trigonal crystals, *J. Comput. Acoust.*, **9**, 1147-1161.

Musgrave, M.J.P., 1970. *Crystal Acoustics*, Holden-Day, San Francisco.

Musgrave, M.J.P., 1985. Acoustic axes in orthorhombic media, *Proc. R. Soc. Lond.*, **A 401**, 131-143.

Pšenčík, I., 1998. Green's functions for inhomogeneous weakly anisotropic media, *Geophys. J. Int.*, **135**, 279-288.

Rümpker, G. & Thomson, C.J., 1994. Seismic-waveform effects of conical points in gradually varying anisotropic media, *Geophys. J. Int.*, **118**, 759-780.

Savage, M.K., Seismic anisotropy and mantle deformation: What have we learned from shear wave splitting?, *Rev. Geophysics*, *37*, 65-106, 1999.

Shuvalov, A.L., 1998. Topological features of the polarization fields of plane acoustic waves in anisotropic media, *Proc. R. Soc. Lond.*, **A 454**, 2911-2947.

Shuvalov, A.L., 2001. On the theory of plane inhomogeneous waves in anisotropic elastic media, *Wave Motion*, **34**, 401-429.

Shuvalov, A.L. & Every, G., 1997. Shape of the acoustic slowness surface of anisotropic solids near points of conical degeneracy, *J. Acoust. Soc. Am.*, **101**, 2381-2383.

Thomsen, L, 1986. Weak elastic anisotropy, *Geophysics*, **51**, 1954-1966.

Vavryčuk, V., 2001. Ray tracing in anisotropic media with singularities, *Geophys. J. Int.*, **145**, 265-276.

Vavryčuk, V., 2003a. Parabolic lines and caustics in homogeneous weakly anisotropic solids, *Geophys. J. Int.*, **152**, 318-334.

Vavryčuk, V., 2003b. Behavior of rays near singularities in anisotropic media, *Phys. Rev. B*, **67**, art. no. 54105.

Vavryčuk, V., 2004. Acoustic axes in triclinic anisotropy, *J. Acoust. Soc. Am.,* submitted.

Wolfe, J.P., 1998. *Imaging Phonons. Acoustic Wave Propagation in Solids*, Cambridge University Press, Cambridge.

Appendix A: Polynomials P_1, Q_1 and R_1

Polynomials P_1, Q_1 and R_1 in (13a-c) are homogeneous polynomials of the sixth order in components of direction vector **n**. They can be expressed as follows:

$$P_1 = n_3 p_{ij} n_1^i n_2^j n_3^{5-i-j},\ Q_1 = n_2 q_{ij} n_1^i n_2^j n_3^{5-i-j},\ R_1 = n_1 r_{ij} n_1^i n_2^j n_3^{5-i-j},$$

where summation over repeated indices is applied. Indices i and j run from 0 to 5 and their sum is less than or equal to 5. Coefficients p_{ij} read

$$p_{50} = b_{56}, \qquad p_{05} = -b_{46},$$
$$p_{20} = -b_{45}, \qquad p_{02} = b_{45},$$
$$p_{32} = b_{24} - b_{14}, \qquad p_{23} = b_{25} - b_{15},$$
$$p_{11} = b_{55} - b_{44}, \qquad p_{22} = 3(-b_{26} + b_{16}),$$
$$p_{40} = b_{45} + b_{36} - b_{16}, \qquad p_{04} = -b_{45} - b_{36} + b_{26},$$
$$p_{41} = b_{46} + b_{25} - b_{15}, \qquad p_{14} = -b_{56} + b_{24} - b_{14},$$
$$p_{30} = -b_{56} + b_{34} - b_{14}, \qquad p_{03} = b_{46} - b_{35} + b_{25},$$
$$p_{21} = -3b_{46} - b_{35} - b_{25} + 2b_{15}, \qquad p_{12} = 3b_{56} + b_{34} - 2b_{24} + b_{14}$$
$$p_{31} = -b_{55} + b_{44} + b_{23} - b_{13} - b_{12} + b_{11}, \qquad p_{13} = -b_{55} + b_{44} + b_{23} - b_{22} - b_{13} + b_{12}$$

other coefficients being zero. Coefficients q_{ij} read

$$q_{50} = b_{56} \qquad q_{00} = -b_{45}$$
$$q_{03} = b_{46} \qquad q_{23} = -b_{46}$$
$$q_{13} = -b_{44} \qquad q_{21} = 3(-b_{35} + b_{15})$$
$$q_{20} = b_{36} - b_{16} \qquad q_{30} = b_{34} - b_{14}$$
$$q_{01} = -b_{46} + b_{35} - b_{25} \qquad q_{10} = -b_{56} + b_{34} - b_{14}$$
$$q_{41} = b_{46} + b_{25} - b_{15} \qquad q_{40} = b_{45} + b_{36} - b_{16}$$
$$q_{02} = b_{45} + b_{36} - b_{26} \qquad q_{32} = -b_{56} + b_{24} - b_{14}$$
$$q_{22} = -3b_{45} - b_{36} - b_{26} + 2b_{16} \qquad q_{12} = 3b_{56} - 2b_{34} + b_{24} + b_{14}$$

$$q_{31} = -2b_{55} + b_{44} + b_{23} - b_{13} - b_{12} + b_{11} \qquad q_{11} = 2b_{55} + b_{44} + b_{23} + b_{13} - b_{12}$$

other coefficients being zero. Coefficients r_{ij} read

$$r_{00} = -b_{45} \qquad r_{05} = b_{46}$$
$$r_{30} = b_{56} \qquad r_{32} = -b_{56}$$
$$r_{31} = -b_{55} \qquad r_{12} = 3(-b_{34} + b_{24})$$
$$r_{02} = b_{36} - b_{26} \qquad r_{03} = b_{35} - b_{25}$$
$$r_{01} = -b_{46} + b_{35} - b_{25} \qquad r_{14} = b_{56} - b_{24} + b_{14}$$
$$r_{04} = b_{45} + b_{36} - b_{26} \qquad r_{10} = -b_{56} + b_{34} - b_{14}$$
$$r_{20} = b_{45} + b_{36} - b_{16} \qquad r_{23} = -b_{46} - b_{25} + b_{15}$$
$$r_{21} = 3b_{46} - 2b_{35} + b_{25} + b_{15} \qquad r_{22} = -3b_{45} - b_{36} + 2b_{26} - b_{16}$$
$$r_{11} = b_{55} + 2b_{44} + b_{23} + b_{13} - b_{12} \qquad r_{13} = b_{55} - 2b_{44} - b_{23} + b_{22} + b_{13} - b_{12}$$

other coefficients being zero. Matrix b_{IJ}, I,J = 1,…,6 is the two-index notation of tensor b_{ijkl} (see Musgrave 1970, eq. 3.13.4).

Appendix B: The Christoffel tensor Γ for weak triclinic anisotropy

Inserting the weak anisotropy expansion, defined in (10) and (11) into the definition of the Christoffel tensor (1), we obtain

$$\Gamma_{11} = (\lambda + 2\mu)n_1^2 + \mu(n_2^2 + n_3^2) + \varepsilon(b_{11}n_1^2 + b_{66}n_2^2 + b_{55}n_3^2 + 2b_{16}n_1n_2 + 2b_{15}n_1n_3 + 2b_{56}n_2n_3)$$
$$\Gamma_{22} = (\lambda + 2\mu)n_2^2 + \mu(n_1^2 + n_3^2) + \varepsilon(b_{66}n_1^2 + b_{22}n_2^2 + b_{44}n_3^2 + 2b_{26}n_1n_2 + 2b_{46}n_1n_3 + 2b_{24}n_2n_3)$$
$$\Gamma_{33} = (\lambda + 2\mu)n_3^2 + \mu(n_1^2 + n_2^2) + \varepsilon(b_{55}n_1^2 + b_{44}n_2^2 + b_{33}n_3^2 + 2b_{45}n_1n_2 + 2b_{35}n_1n_3 + 2b_{34}n_2n_3)$$
$$\Gamma_{12} = (\lambda + \mu)n_1n_2 + \varepsilon[b_{16}n_1^2 + b_{26}n_2^2 + b_{45}n_3^2 + (b_{12} + b_{66})n_1n_2 + (b_{14} + b_{56})n_1n_3 + (b_{25} + b_{46})n_2n_3]$$

$$\Gamma_{13} = (\lambda + \mu)n_1n_3 + \varepsilon[b_{15}n_1^2 + b_{46}n_2^2 + b_{35}n_3^2 + (b_{14} + b_{56})n_1n_2 + (b_{13} + b_{55})n_1n_3 + (b_{45} + b_{36})n_2n_3]$$
$$\Gamma_{23} = (\lambda + \mu)n_2n_3 + \varepsilon[b_{56}n_1^2 + b_{24}n_2^2 + b_{34}n_3^2 + (b_{25} + b_{46})n_1n_2 + (b_{36} + b_{45})n_1n_3 + (b_{23} + b_{44})n_2n_3]$$

Appendix C: The linearized Khatkevich equations

Using eqs (15a-b), we obtain the following components of submatrix $\mathbf{A}^{(i)}$ and of vector $\mathbf{c}^{(i)}$ specified for the *i*th acoustic axis:

$$A_1^1 = n_3\left(n_1^4 - n_1^2 n_3^2 - n_2^4 + n_2^2 n_3^2\right)$$

$$A_2^1 = n_2\left(n_1^4 - 3n_1^2 n_3^2 - n_2^4 + n_2^2 n_3^2\right)$$

$$A_3^1 = n_1 n_2 n_3\left(-n_1^2 - n_2^2 + n_3^2\right)$$

$$A_4^1 = n_1\left(n_1^4 - n_1^2 n_3^2 - n_2^4 + 3n_2^2 n_3^2\right)$$

$$A_5^1 = n_1^3 n_2 n_3$$

$$A_6^1 = -n_1 n_2^3 n_3$$

$$A_7^1 = n_1\left(n_1^2 n_2^2 + n_1^2 n_3^2 + n_2^4 - n_2^2 n_3^2\right)$$

$$A_8^1 = n_1 n_2^2\left(-n_1^2 - n_2^2 + 2n_3^2\right)$$

$$A_9^1 = n_1^2 n_2\left(n_1^2 + n_2^2 - 2n_3^2\right)$$

$$A_{10}^1 = n_2\left(-n_1^4 - n_1^2 n_2^2 + n_1^2 n_3^2 - n_2^2 n_3^2\right)$$

$$A_{11}^1 = n_1^2 n_3\left(n_1^2 - 3n_2^2\right)$$

$$A_{12}^1 = n_2^2 n_3\left(3n_1^2 - n_2^2\right)$$

$$A_{13}^1 = n_1 n_2 n_3\left(n_1^2 - n_2^2\right)$$

$$A_1^2 = n_3\left(n_1^4 - 3n_1^2 n_2^2 + n_2^2 n_3^2 - n_3^4\right)$$

$$A_2^2 = n_2\left(n_1^4 - n_1^2 n_2^2 + n_2^2 n_3^2 - n_3^4\right)$$

$$A_3^2 = 2n_1 n_2 n_3\left(-n_1^2 + n_3^2\right)$$

$$A_4^2 = n_1\left(n_1^4 - n_1^2 n_2^2 + 3n_2^2 n_3^2 - n_3^4\right)$$

$$A_5^2 = n_1^3 n_2 n_3$$

$$A_6^2 = 0$$

$$A_7^2 = n_1\left(n_1^2 n_2^2 + n_1^2 n_3^2 - n_2^2 n_3^2 + n_3^4\right)$$

$$A_8^2 = -n_1 n_2^2\left(n_1^2 + n_3^2\right)$$

$$A_9^2 = n_1^2 n_2\left(n_1^2 - 3n_3^2\right)$$

$$A_{10}^2 = n_2\left(-n_1^4 + n_3^4\right)$$
$$A_{11}^2 = n_1^2 n_3\left(n_1^2 - 2n_2^2 + n_3^2\right)$$
$$A_{12}^2 = n_2^2 n_3\left(n_1^2 + n_3^2\right)$$
$$A_{13}^2 = n_1 n_2 n_3\left(n_1^2 + n_3^2\right)$$

$$\mathbf{A}^{(i)} = \begin{bmatrix} A_1^1 & A_2^1 & A_3^1 & A_4^1 & A_5^1 & A_6^1 & A_7^1 & A_8^1 & A_9^1 & A_{10}^1 & A_{11}^1 & A_{12}^1 & A_{13}^1 \\ A_1^2 & A_2^2 & A_3^2 & A_4^2 & A_5^2 & A_6^2 & A_7^2 & A_8^2 & A_9^2 & A_{10}^2 & A_{11}^2 & A_{12}^2 & A_{13}^2 \end{bmatrix}$$

$$\mathbf{c}^{(i)} = \begin{bmatrix} -n_1 n_2 n_3\left(n_1^2 + n_2^2 - n_3^2\right) \\ -n_1 n_2 n_3\left(n_1^2 - n_2^2 + n_3^2\right) \end{bmatrix}$$

where superscript i denotes the sequential number of the acoustic axis, and **n** is the direction vector of this axis. Inserting submatrices $\mathbf{A}^{(i)}$ and vectors $\mathbf{c}^{(i)}$ into (22) we construct matrix **A** and vector **c** required in the system of linear equations (23).

Appendix D: The linearized Darinskij equations

Using eq. (31), we obtain the following components of submatrix $\mathbf{A}^{(i)}$ and of vector $\mathbf{c}^{(i)}$ specified for the *i*th acoustic axis:

$$A_1^1 = 2n_1 n_2\left(-4n_1^4 - 4n_1^2 n_2^2 + 5n_1^2 - 1\right)$$
$$A_2^1 = 2n_1 n_3\left(4n_1^2 n_2^2 + n_1^2 - 1\right)$$
$$A_3^1 = -4n_1^6 - 4n_1^4 n_2^2 + 8n_1^4 + 3n_1^2 n_2^2 - 5n_1^2 - n_2^2 + 1$$
$$A_4^1 = 2n_2 n_3\left(4n_1^4 - 3n_1^2 + 1\right)$$
$$A_5^1 = n_1^2\left(n_1^4 - 2n_1^2 + 1\right)$$
$$A_6^1 = n_2^2\left(n_1^2 n_2^2 + n_1^2 + n_2^2 - 1\right)$$
$$A_7^1 = 4n_1^2 n_2 n_3\left(-n_1^2 + 1\right)$$
$$A_8^1 = 2n_2 n_3\left(-2n_1^2 n_2^2 - n_1^2 - 2n_2^2 + 1\right)$$
$$A_9^1 = 2n_1 n_3\left(-2n_1^4 + 3n_1^2 - 1\right)$$
$$A_{10}^1 = -4n_1^3 n_2^2 n_3$$

$$A_{11}^1 = 2n_1n_2\left(-2n_1^4 + 3n_1^2 - 1\right)$$
$$A_{12}^1 = 2n_1n_2\left(-2n_1^2n_2^2 - n_1^2 + 1\right)$$
$$A_{13}^1 = 2n_1^2n_2^2\left(-n_1^2 + 1\right)$$

$$A_1^2 = 2n_1n_2\left(-4n_1^2n_2^2 - 4n_2^4 + 5n_2^2 - 1\right)$$
$$A_2^2 = 2n_1n_3\left(4n_2^4 - 3n_2^2 + 1\right)$$
$$A_3^2 = -4n_1^4n_2^2 - 4n_1^4 - 4n_1^2n_2^4 - n_2^4 + 4n_1^2 + 2n_2^2 - 1$$
$$A_4^2 = 2n_2n_3\left(4n_1^2n_2^2 + n_2^2 - 1\right)$$
$$A_5^2 = n_1^2\left(n_1^2n_2^2 + n_1^2 + n_2^2 - 1\right)$$
$$A_6^2 = n_2^2\left(n_2^4 - 2n_2^2 + 1\right)$$
$$A_7^2 = -4n_1^2n_2^3n_3$$
$$A_8^2 = 2n_2n_3\left(-2n_2^4 + 3n_2^2 - 1\right)$$
$$A_9^2 = 2n_1n_3\left(-2n_1^2n_2^2 - 2n_1^2 - n_2^2 + 1\right)$$
$$A_{10}^2 = 4n_1n_2^2n_3\left(-n_2^2 + 1\right)$$
$$A_{11}^2 = 2n_1n_2\left(-2n_1^2n_2^2 - n_2^2 + 1\right)$$
$$A_{12}^2 = 2n_1n_2\left(-2n_2^4 + 3n_2^2 - 1\right)$$
$$A_{12}^2 = 2n_1^2n_2^2\left(-n_2^2 + 1\right)$$

$$\mathbf{A}^{(i)} = \begin{bmatrix} A_1^1 & A_2^1 & A_3^1 & A_4^1 & A_5^1 & A_6^1 & A_7^1 & A_8^1 & A_9^1 & A_{10}^1 & A_{11}^1 & A_{12}^1 & A_{13}^1 \\ A_1^2 & A_2^2 & A_3^2 & A_4^2 & A_5^2 & A_6^2 & A_7^2 & A_8^2 & A_9^2 & A_{10}^2 & A_{11}^2 & A_{12}^2 & A_{13}^2 \end{bmatrix}$$

$$\mathbf{c}^{(i)} = \begin{bmatrix} 4n_1^4n_2^2 + n_1^4 + 4n_1^2n_2^4 + 4n_2^4 - 2n_1^2 - 4n_2^2 + 1 \\ 4n_2^6 + 4n_1^2n_2^4 - 8n_2^4 - 3n_1^2n_2^2 + n_1^2 + 5n_2^2 - 1 \end{bmatrix}$$

where superscript i denotes the sequential number of the acoustic axis, and $\mathbf{n}$ is the direction vector of this axis. Inserting submatrices $\mathbf{A}^{(i)}$ and vectors $\mathbf{c}^{(i)}$ into (22) we construct matrix $\mathbf{A}$ and vector $\mathbf{c}$ required in the system of linear equations (23).